

# ANALYSIS OF POTENTIAL HELICOPTER VIBRATION REDUCTION CONCEPTS

Anton J. Landgrebe  
Manager, Aeromechanics Research

and

Mark W. Davis  
Associate Research Engineer, Aeromechanics Research

United Technologies Research Center  
East Hartford, Connecticut

## Abstract

Several recent helicopter vibration reduction research programs of the United Technologies Research Center (UTRC) are described. Results of analytical investigations to develop, understand, and evaluate potential helicopter vibration reduction concepts are presented in the following areas: identification of the fundamental sources of vibratory loads, blade design for low vibration, application of design optimization techniques, active higher harmonic control, blade appended aeromechanical devices, and the prediction of vibratory airloads. Primary sources of vibration are identified for a selected four-bladed articulated rotor operating in high speed level flight. The application of analytical design procedures and optimization techniques are shown to have the potential for establishing reduced vibration blade designs through variations in blade mass and stiffness distributions, and chordwise center-of-gravity location. Analytical evaluation of a computerized generic active controller for implementing higher harmonic control indicates the potential for good controller performance and extensive fuselage vibration reduction with low pitch amplitudes for three controller approaches investigated. Exploratory evaluation of a passive tuned blade tab concept indicates considerable sensitivity of vibratory load alleviation to design parameters with an improvement in inplane hub excitation but an increase in vertical excitation. The prediction of vibratory airloads, attributable to rotor/wake, rotor/fuselage, and rotor/empennage interactional aerodynamics, is also described.

## Introduction

For future helicopters to reach their full potential, significant reduction in vibration must be accomplished. Helicopter vibration is becoming an increasingly important consideration because of requirements for crew and passenger comfort as well as increased reliability of structural components and on-board electronic equipment. A vibration-free weapons platform is also a requirement for

some military helicopters. As helicopters are required to fly more at both faster cruise speeds and slow "transition" speeds for nap-of-the-earth flying, the need to minimize vibration becomes more important, and it becomes necessary to consider alternative and complementary approaches for vibration reduction.

Helicopter vibration research has been a primary activity at the United Technologies Research Center (UTRC) for the past six years. Various helicopter vibration related programs involving analytical investigation have been conducted in the following areas:

- Blade design for low vibration
- Design optimization techniques applicable to vibration reduction
- Active higher harmonic control for vibration alleviation
- Blade appended devices for vibration alleviation
- Prediction of vibratory airloads (rotor, fuselage, empennage).

In the Ref. 1 analytical investigation, rotor vibratory response and loads transmitted to the fuselage were predicted and analyzed to determine the relative contributions and sources of the various components of blade force excitation. Primary sources of vibration were identified for a selected four-bladed articulated rotor operating in high speed level flight. Subsequently, blade modal shaping (Ref. 2), frequency placement, structural and aerodynamic coupling, and intermodal cancellation were investigated to systematically identify and evaluate blade design parameters that influence vibratory airloads, blade modal response, hub loads, and fuselage vibration. Through variations in blade mass distribution, stiffness distribution and chordwise center-of-gravity location, blade designs were developed with predicted reductions in vibration. These designs remain to be validated by test.

An automated optimization procedure is being developed at UTRC for the rotor blade design

Presented at the American Helicopter Society and NASA Ames Research Center 2nd Decennial Specialists' Meeting on Rotorcraft Dynamics, November 7-9, 1984.

process. A simplified approach for minimizing vibration (Refs. 1, 2) has been developed and applied (Ref. 3). A modal analysis was used to calculate key vibration parameters. Through frequency placement and modal shaping with a constrained optimization program, COPES/CONMIN, (Refs. 4, 5) a blade design was determined for reduced fuselage vibration. A forced response aeroelastic analysis (Ref. 6) was used in the process to identify modes, the desired frequency placement and modal shaping criteria, and to perform a final calculation of the vibration characteristics of the new blade designs.

A computerized generic active controller was developed for alleviating helicopter vibration by closed-loop implementation of higher harmonic control (HCC) (Refs. 7, 8). This controller provides the unique capability to readily define and evaluate many different algorithms by selecting from three controller approaches (deterministic, cautious, and dual), two linear system models (local and global), and several methods of limiting control. A non-linear aeroelastic rotor analysis (Ref. 6) was used to evaluate alternative controller configurations as applied to a four-bladed H-34 rotor mounted on the NASA-Ames Rotor Test Apparatus used to represent the fuselage. It will be shown that excellent controller performance was predicted for all three controller approaches for steady flight conditions having moderate to high values of forward velocity and rotor thrust. Reductions in vibration from 75 to 95 percent were predicted with HCC pitch amplitudes of less than one degree. Good transient vibration alleviation was also predicted for short duration maneuvers involving a sudden change in collective pitch.

Analytical evaluations of aeroelastic devices appended to helicopter rotor blades have been conducted to determine their potential for reducing hub shears and vibratory control loads (Ref. 9). The results for a passive tuned tab shall be discussed.

The development of methodology to predict vibratory blade airloads has proceeded at UTRC along with the determination of primary airload sources. Wake, airflow, and airload methodology have advanced for both low and high speed flight (Refs. 10-19). For example, a first level generalization of the forward flight rotor wake has recently been formulated for use in unsteady airload calculations (Refs. 10, 11, 12). Synthesization procedures for incorporating unsteady airfoil test data in rotor aeroelastic response methods have been developed (Ref. 18). Also, methodology for predicting vibratory airload excitation at tail surfaces due to the rotor wake has been developed and initial validation has been performed (Ref. 19). The aerodynamic interaction of the fuselage on the rotor vibratory airloads has been analytically demonstrated (Ref. 17). Development of a computer method for predicting the induced unsteady vibratory excitation of the rotor wake on the fuse-

lage is in progress.

The aforementioned investigations are described in the following sections.

#### Blade Design for Vibration Reduction

An analytical investigation was conducted to develop an understanding of the importance and role played by blade design parameters in rotor vibratory response and to design an advanced blade for reduced vibration based upon this understanding. This investigation was conducted at UTRC by Taylor (Ref. 1). Various design approaches were examined for a four-bladed articulated rotor operating at a high-speed, level flight condition. Blade modal shaping, frequency placement, structural and aerodynamic coupling, and intermodal cancellation were investigated to systematically identify and evaluate blade design parameters that influence blade vibratory airloads, blade modal responses, hub loads, and fuselage vibration.

The baseline rotor system selected for the investigation was a four-bladed articulated rotor system, similar in design to the Sikorsky S-76 rotor system, but without vibration alleviation devices and tip sweep. Tip sweep can provide vibration alleviation through aeroelastic coupling between the blade flatwise and blade torsion modes. However, it was decided to omit tip sweep from the baseline blade design to study the potential of improving the vibration characteristics of a basic rectangular planform blade. A complete set of baseline blade properties is presented in Ref. 1. The blade spanwise mass distribution for the baseline and modified blade designs will be presented in the following section on blade design optimization. Some of the relevant properties of the baseline blade are the blade twist (-10 deg, nonlinear), blade weight (100 lb) and non-dimensionalized natural frequencies (flatwise modes: rigid body = 1.03 per rev, first elastic = 2.75 per rev, second elastic = 4.9 per rev; edgewise modes: rigid body = 0.26 per rev, first flexible = 4.7 per rev; torsion mode: first elastic = 5.30 per rev). The baseline blade pitch axis, elastic axis, aerodynamic center, and center-of-gravity (CG) were nominally located at the 25 percent chord (outboard, CG was at 26%). The flight condition selected was a high speed cruise condition of 160 kt. A 10,800 lb rotor lift and an 1190 lb propulsive force were selected to be representative for a helicopter the size of the S-76.

The analytical simulation used for this study was the G400 analysis documented in Ref. 6. This computer analysis is based on the Galerkin method and uses precalculated uncoupled normal blade modes. A time history solution of airloads, blade responses, and vibratory blade hub forces and moments due to the rotor are calculated based on modal coupling within the analysis. For this study, the fuselage vibrations were determined by means of a measured S-76 mobility transfer matrix

between the hub loads and vibrations at several locations in the airframe. This approach was used to separate rotor design effects from hub impedance and airframe dynamic effects in the analysis. Uniform inflow was used in this initial exploratory study to model the rotor downwash for the high speed flight condition. The influence of variable inflow on vibratory airloads will be included in subsequent blade design studies.

In order to design blades for reduced helicopter vibration, it is necessary to first acquire a fundamental understanding of the interrelationship of the fuselage vibrations, the hub loads in the fixed system, the blade root loads in the rotating system, the blade vibratory response, and the blade airloads. It is then necessary to identify the primary contributors of the various harmonic modal components to vibratory excitation. As indicated in Fig. 1, for a helicopter with a four-bladed articulated rotor, the predominant 4P (4 per rev) cockpit and cabin vibrations are mainly produced by the 4P vertical and inplane (lateral and longitudinal) hub forces, since for a low-offset articulated rotor the 4P moment contribution is of secondary importance. For a four-bladed rotor in a steady-state condition, the 4P hub fixed system vertical shear results directly from the azimuthal summation of the 4P blade root rotating vertical shear from all blades. When the contributions of all four blades are summed in the fixed system, the 4P hub fixed system inplane shears result from the summation of 3P and 5P blade root rotating inplane shears. As indicated in Fig. 1, the contribution of the 5P inplane shears were found early in this investigation to be small relative to the 3P contribution.

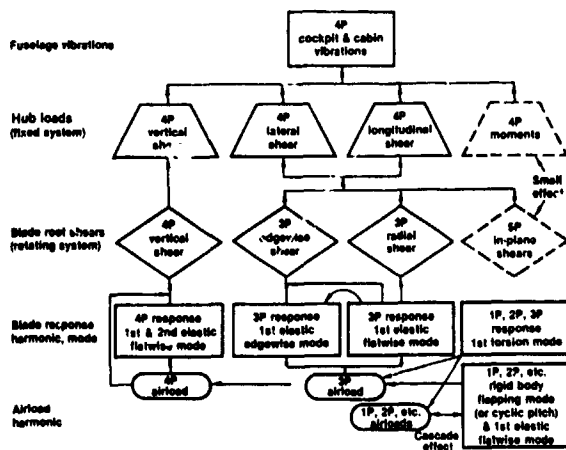


Fig. 1. Primary Contributors to Helicopter Vibrations (4-Bladed Articulated Rotor, High Speed Flight)

With the awareness of the above information at the beginning of the investigation, the analytical study was directed toward identifying the primary blade response contributors and related airload harmonics, as will be discussed. With this information and an understanding acquired from sensitiv-

ity studies, several blades were designed and reported in Ref. 1 which resulted in lower predicted vibration levels. Results for the baseline and the two final modified blade designs (Designs A and B) are summarized herein. It should be noted that these blade designs were achieved via closed-loop optimization techniques as discussed in the next section.

The predicted 4P hub loads and fuselage vibrations for the baseline and two modified blade designs are presented in Figs. 2 and 3, respectively. For the baseline articulated rotor, the vibratory hub load components with the most influence on fuselage vibration are, in order of importance, the longitudinal, lateral, and vertical shears. On other helicopters having a different mobility matrix, the vertical shear may be more

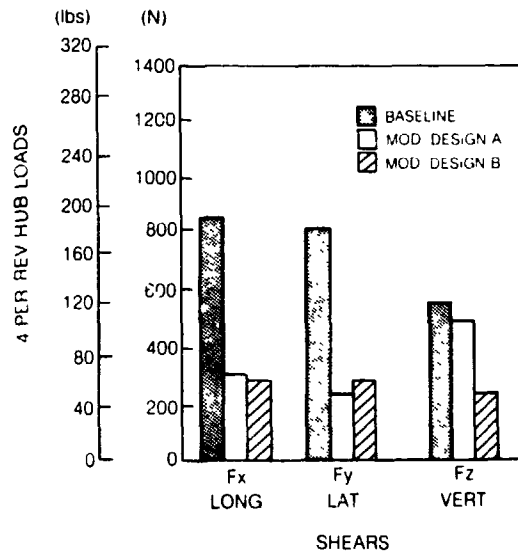


Fig. 2. Predicted Vibratory Fixed-System Hub Loads for the Baseline and Modified Blade Designs (V = 160 kt)

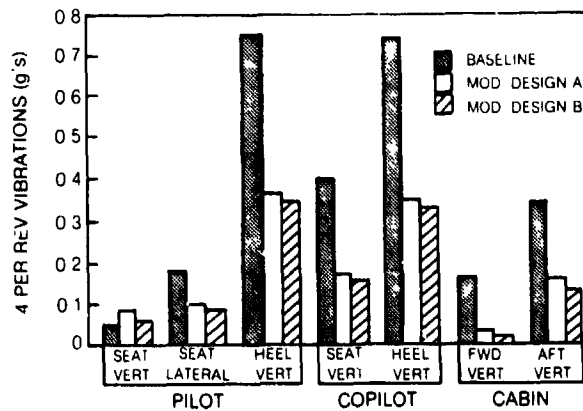


Fig. 3. Predicted 4 Per Rev Fuselage Vibrations for the Baseline and Modified Blade Designs (V = 160 kt)

important than the inplane shears. For hingeless or bearingless rotors, the hub moments can become important. Of the fuselage vibrations shown in Fig. 3, the dominant vibrations for the aircraft studied are the heel-slide vibrations for the pilot and copilot. Important vibrations are those affecting crew and passenger comfort. Thus, it was considered a good objective to reduce the cockpit seats and cabin vibrations to approximately 0.1 g while reducing the heel-slide vibrations to the extent possible. As shown in Fig. 3, the predicted fuselage vibrations for modified Designs A and B are lower by about 50 percent (except the small pilot seat vertical vibration) compared to the baseline vibrations. Of particular importance are the seat and cabin vibrations which are approaching the 0.1 g level. These results indicate that acceptable seat and cabin vibration levels can be attained, at least theoretically, by improved blade design and without the use of vibration treatment equipment (bifilars, absorbers, etc.). The vibratory hub loads that produced these vibrations are shown in Fig. 2 to also have been reduced significantly.

To achieve the vibration levels predicted for Designs A and B, the following modifications were made to the baseline blade. For Design A, a combination of blade spanwise mass redistribution and increased edgewise blade stiffness was used to change the blade mode shapes and increase the uncoupled frequencies of the first elastic flatwise and edgewise modes from 2.75 to 3.4 per rev and 4.8 to 5.8 per rev, respectively. Modal shaping techniques described in Refs. 1 and 2 and summarized in the next section on optimization were applied in addition to frequency placement techniques. A small change in blade weight (100 to 104 lb) resulted. Increasing the flatwise frequency to 3.4 per rev improved the inplane shear, but did not significantly reduce the vertical shear, as shown in Fig. 2. For Design B, the generalized airload producing a large response of the first flatwise mode was decreased by moving forward the CG location of the outer 20 percent of the blade from 26 to 24 percent of the chord. The basis for these design changes are discussed below.

In order to understand the source of the rotating blade root shears, the G400 analysis was used to decompose the vertical and inplane shear components (edgewise and radial) into the individual contributing components. This is exemplified in Fig. 4 for the 3P rotating edgewise shear transmitted to the hub by the baseline blade. The force vectors are presented in polar format showing the amplitude and phase of the total shear and contributing components. It is important to note that the two principal components due to rigid body motion (rigid flapping coriolis and lag inertia) vectorially combine with the drag component to form a small contribution to the total.

As a result of this cancellation effect, the elastic blade components of shear acquire a primary role. In particular, the elastic flatwise inertia

component is the predominant contributor to the 3P edgewise shear. This component arises from the flatwise mode coupling with the edgewise mode associated with blade twist and collective pitch. In Fig. 5, it is shown that the elastic flatwise contribution is also important to the radial shear

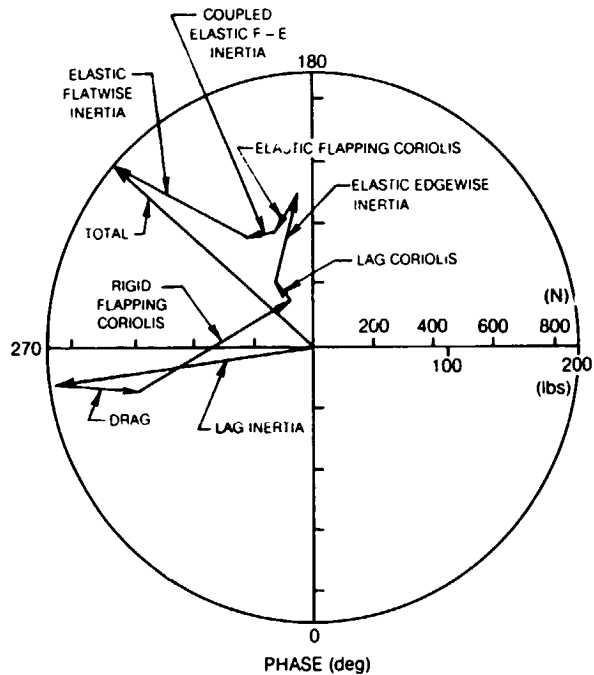


Fig. 4. Predicted 3 Per Rev Rotating Blade Root Edgewise Shear for the Baseline Blade ( $V = 160$  kt)

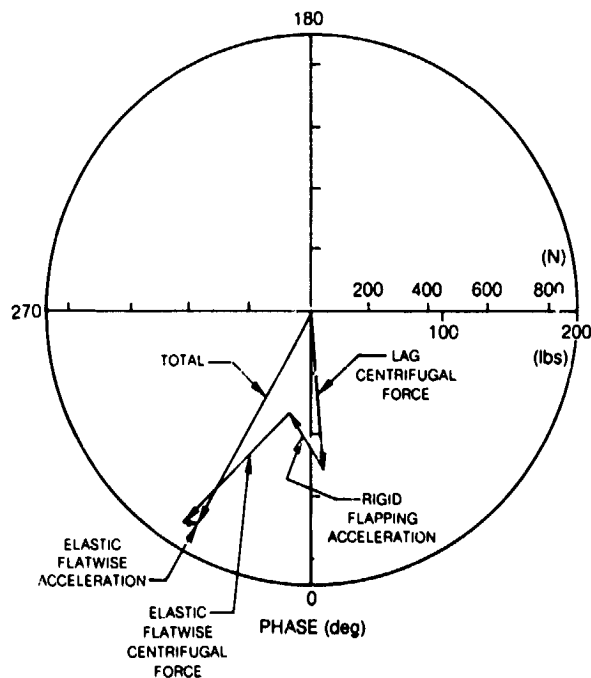


Fig. 5. Predicted 3 Per Rev Rotating Blade Root Radial Shear for the Baseline Blade ( $V = 160$  kt)

ORIGINAL PAGE IS  
OF POOR QUALITY

component. It thus became evident that significant intermodal coupling occurs, and reduction of the vibratory inplane hub loads is heavily dependent upon reduction in the response of the first elastic flatwise mode in addition to the first elastic edgewise mode as summarized in Fig. 1. It was also noted that significant vectorial cancellation of components of shear due to phase as well as amplitude differences occurred. Thus, the predicted total shears are very sensitive to the accuracy of the simulation analysis.

Also, it is described in Ref. 1 that significant interharmonic and intermodal coupling occurs between the blade flatwise response and the airloads. This is indicated in Fig. 1 as a "cascade effect" in which modal motions at one harmonic induce modal motions at other harmonics through the coupling with the harmonics of airloads. For forward flight, the one per rev airloads created by flapping (or cyclic pitch), required for aircraft trim, result in one per rev response of all blade modes. The resulting one per rev motions create 2, 3, 4, and 5 per rev response of the blade modes and so on. The end result for the rotor investigated was that significant 3P and 4P airloads were generated which excited the important 3P and 4P responses shown in Fig. 1. The rotor thus largely excites itself through the blade motion-airload cascade effect. Also, as will be described, harmonic inflow and airloads due to rotor wake effects provide vibratory excitation which, for steady level flight, is large at low speeds and less at high speeds.

For modified Design A, the reduction of the 3P root edgewise shear and its components is shown in Fig. 6 (note the scale change relative to Fig. 4). The important elastic inertia components were substantially reduced. The reduction in the predicted 3P and 4P modal responses are shown in Fig. 7. Although the inplane hub shear was largely reduced for Design A, the vertical hub shear was not, as shown in Fig. 2. This was attributed to an over reduction of the second elastic flatwise mode contribution and the fact that the second mode provided phase cancellation with the first mode. Although cancellation between the two modal contributions to vertical shear could have been pursued by blade design retuning with mass and stiffness variations, it was decided not to depend upon this cancellation due to intermodal phasing which could change with rotor configuration or flight condition. Instead, the 4P vertical shear was reduced, as reported in Ref. 1, by changing the blade outboard center-of-gravity location to reduce the generalized airload.

Changing the center-of-gravity (CG) location, over the outer blade region, from 26 to 24 percent of the chord moved the CG forward of the elastic axis (EA) and influenced the blade airloads through inertial coupling between the blade flatwise and torsion responses. The predicted change in the torsion response time history around the azimuth for this modified blade Design B is shown in Fig.

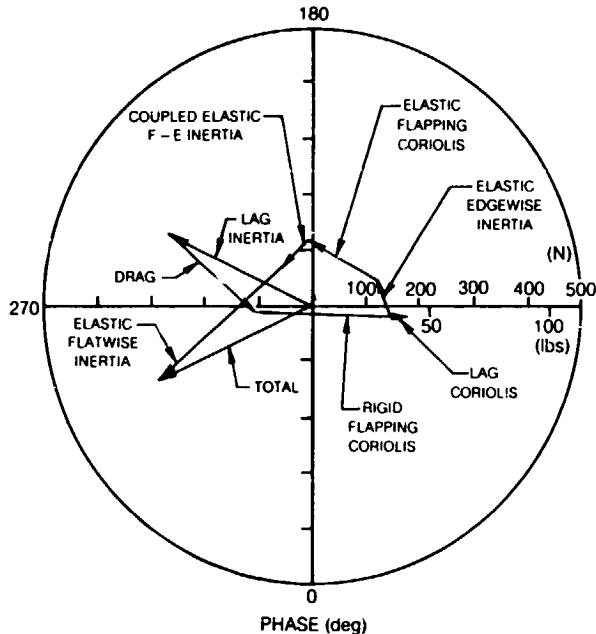


Fig. 6. Predicted 3 Per Rev Rotating Blade Root Edgewise Shear for Modified Blade Design A (V = 160 kt)

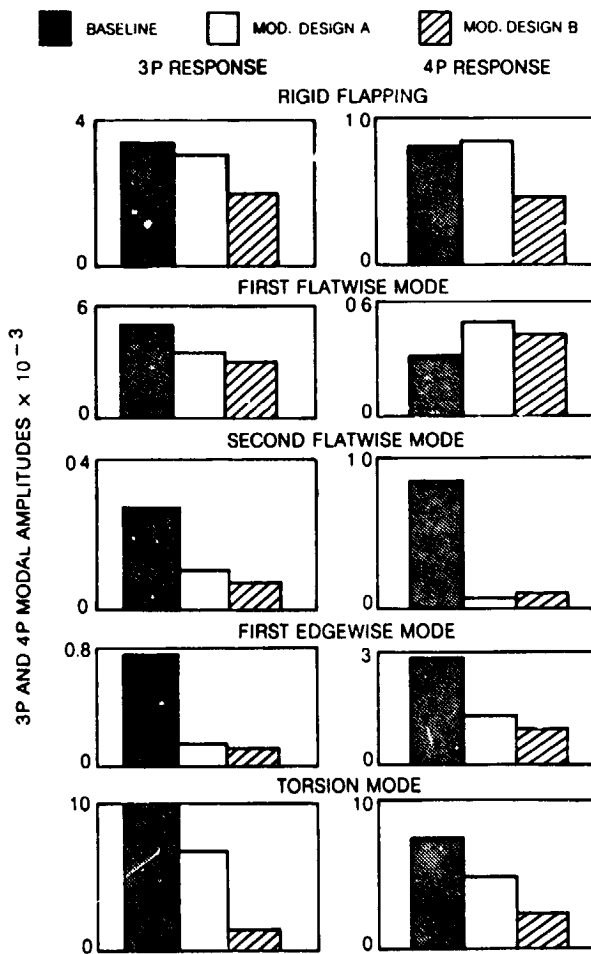


Fig. 7. Predicted 3P and 4P Modal Response for the Baseline and Modified Blade Designs (V = 160 kt)

8. For the baseline design, the torsion response is characterized by a strong nose-down deflection on the rotor advancing side. For blade Design B, the nose-down response on the advancing side was eliminated leaving a waveform that consists of a 1P response, maximum nose down at 180 degrees azimuth, plus smaller contributions of higher harmonics. The mechanism involved in this phenomenon is the CG-EA offset. When the blade tip bends downward on the advancing side, a forward CG induces a nose-up torsion increase on the blade near the blade tip. This moment counteracts the nose-down aerodynamic pitching moment due to high Mach number on the advancing side. It was found that, when the CG is moved further forward, the increased advancing side nose-up response can produce increased vibration. Blade tip sweep is an alternate approach that has been used to reduce the advancing side vibratory airloads through blade aeroelastic torsional deformation.

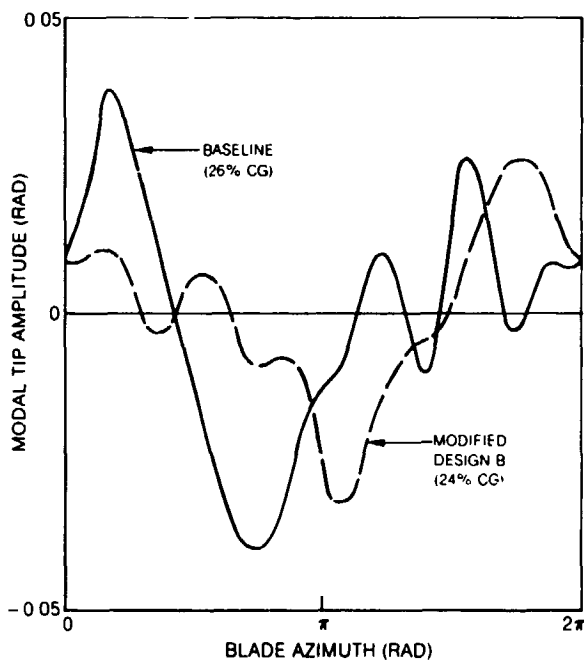


Fig. 8. Predicted Effect of Outboard CG Location on Blade Torsion Mode Response ( $V = 160$  kt)

The reduction of the torsion mode response of modified Design B is shown in Figs. 7 and 8. The reduction of the 4P vertical shear relative to the baseline and Design A blade levels is shown in Fig. 2. Relative to Design A levels, a small further reduction in 4P fuselage vibration is indicated at all fuselage locations in Fig. 3. The resulting fuselage vibration are generally about half the baseline blade levels.

In summary, the predicted results for the modified blade designs in Ref. 1 indicate the potential for substantially reducing helicopter vibration by viable changes in blade design. Further study in the area of blade design for vibration

could possibly result in rotors with vibration levels that are acceptable without the use of vibration alleviation devices or higher harmonic control. However, it is recognized that the predicted results have not yet been substantiated with test. Due to the absence of a systematic, consistent set of experimental data for vibratory blade, hub, and fuselage loads, the G400 analysis, like other rotor aeroelastic analyses, has not been validated for vibration prediction. The high degree of interharmonic and intermodal coupling and the predicted cancellation effects of large components of hub loads make the results sensitive to the prediction accuracy of the analysis for the individual components. In fact, differences of the predictions with the vibration results of preliminary exploratory tests at Sikorsky have been noted. The provision of a model test rig to systematically and accurately measure vibratory hub loads is currently being pursued at UTRC to validate computer codes and evaluate new blade designs for vibration. Also, application of blade design techniques for vibration to other rotor types (hingeless, bearingless) is underway and application to other flight conditions (particularly low speed) with variable inflow is planned. The inclusion of design optimization techniques has been initiated as described below.

#### Rotor Blade Design Optimization for Vibration

The optimization approach discussed below is part of an ongoing effort at UTRC to develop a general automated procedure for rotor blade design. This procedure can be used to determine the necessary geometric, structural, and material properties of a rotor system to achieve desired design objectives relating to vibration, stress, and aerodynamic performance. This section concentrates on the approach used for helicopter vibration summarized in Ref. 3. Based on the analytical studies discussed above, a simplified vibration analysis has been developed for use in conjunction with a forced response analysis in the optimization process. This simplified analysis significantly improves the efficiency of the design process.

#### Optimization Approach

As shown in Fig. 9, the approach for rotor blade design has been formulated as three separate component optimization problems concerned with areas such as vibration, stress, and aerodynamic performance. Appropriate constraint functions are formulated to account for the influence of design changes in areas other than those of primary concern for a given problem. After gaining experience with each component problem, the goal is to develop a completely integrated approach to optimize on several design considerations simultaneously. Based on experience with the individual optimization problems, it will be possible to better formulate an integrated and efficient overall approach. Furthermore, experience will be gained as to the design variables having the largest impact on each individual problem, the

tradeoffs to be expected between various design considerations, and the capability to meet specified design criteria for a given problem.

Figure 9 also shows a few potential design parameters that might be used for the optimization problems. These include: blade geometrical properties, primarily associated with aerodynamic performance; material properties, generally associated with blade stress; and structural properties, associated with vibration and stress. In this section, only the vibration problem is considered. The design parameters used are mass and bending stiffness distributions along the blade.

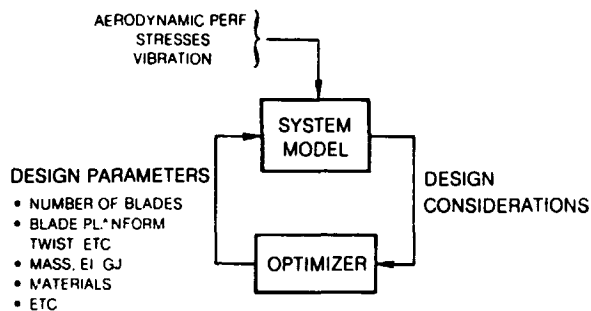


Fig. 9. Overall Approach for Rotor Blade Design Optimization

Figure 10 outlines the approach to be used for helicopter vibration. In order to achieve the computer efficiency required of any useful design optimization tool, a simplified vibration analysis is used in the primary or inner loop to develop the vibration parameters and other criteria to be optimized. Since this simplified analysis may be performed many times faster than the forced response analysis, the potential savings in time is significant for the many iterations that may be required by any constrained optimization program. The forced response analysis G400 is then used to verify the vibration characteristics of the new blade design in the outer optimization loop, where closed-loop optimization can also be performed.

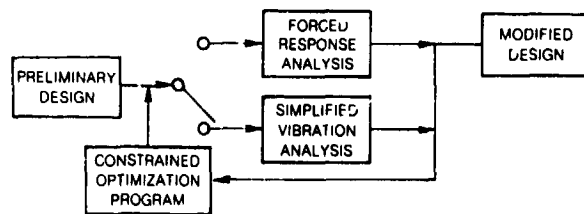
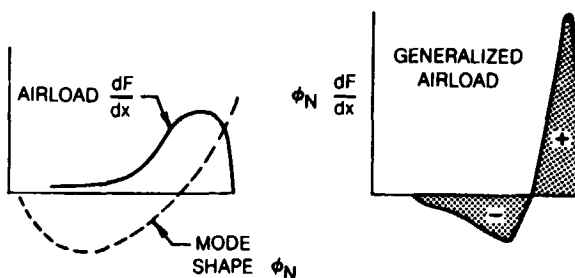


Fig. 10. Optimization Approach for Vibration

The simplified vibration analysis is based on the assumption that appropriate modal parameters can be defined that indirectly relate changes in vibration characteristics to changes in blade

design. Traditionally, frequency placement has been used to minimize vibration response. As discussed above, modal shaping has also been shown to be important, and associated parameters have been identified as indicators of rotor blade vibration characteristics. In particular, it has been predicted that vibration can be reduced by minimizing certain weighted modal integrals. In studies performed to date, polynomial approximations to the airload distribution have been used as weightings in the modal integrals. As shown conceptually in Fig. 11, mode shaping is accomplished by driving these generalized airloads to zero to desensitize the blade to vibratory airloading.



- DESENSITIZE BLADE TO VIBRATORY AIRLOADS BY SHAPING OF CRITICAL MODES:

$$\text{GENERALIZED AIRLOAD} = \int \phi_N \frac{dF}{dx} dx - 0$$

Fig. 11. Modal Shaping Design Concept

Figure 12 shows a more detailed schematic of the inner optimization loop presented in Fig. 10. A blade eigensolution analysis (E159) is used to calculate blade natural frequencies and mode shapes for a given set of design variables. This information and the assumed airload distributions are used to calculate the appropriate modal integrals and the difference between the actual and optimum modal frequencies. Frequency placement and modal shaping are accomplished by simultaneously driving these parameters to zero via minimization of a quadratic performance index that consists of the weighted sum of the squares of each vibration parameter. The weighting matrix,  $W_2$ , is used to reflect the relative importance of each vibration parameter.

The constrained optimization program used for the results presented in this paper is COPES/CONMIN (Refs. 4 and 5), which is based on the Method of Feasible Directions. This program minimizes the performance index in an iterative manner. At each step, it attempts to satisfy all specified constraints, which may be either explicit or implicit functions of the design variables. As shown by the dashed line in Fig. 12, blade frequencies and modal integrals can also be included as constraints rather than added to the performance index. Based on gradient and functional information for the objective and constraint functions, COPES/CONMIN

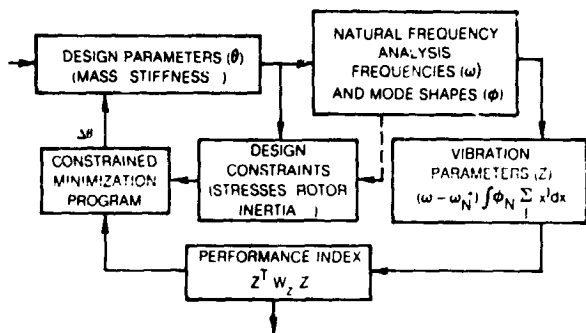


Fig. 12. Automated Design Procedure for Vibration Based on Simplified Approach

calculates necessary changes in the design variables to further reduce the performance index at the current iteration. The necessary gradients are calculated by finite differences.

#### Analytical Results

The simplified approach outlined in Figs. 10 through 12 was used to optimize the previously described baseline articulated rotor operating at a steady 160 kt flight condition. Thirty (30) design variables were used to tailor three selected modes. The design variables consisted of the flatwise and edgewise bending stiffnesses and the mass at each of ten (10) spanwise blade stations. Optimum frequency and modal integral values were specified for three selected modes to give a total of six (6) vibration parameters to be reduced. As discussed in the last section on blade design for reduced vibration, G400 was used to identify the key modes and the associated frequency placement and modal shaping criteria for the articulated rotor investigated. The three modes selected were the first and second elastic flatwise modes and the first elastic edgewise mode. These modes were selected to reduce the response of the two inplane hub shears, which were identified as primary contributors to fuselage vibration in this rotorcraft. The modal integral used for each mode included a cubic weighting function of the blade spanwise location ( $x$ ) to approximate the airloading for this high speed flight condition.

Analytical studies with G400 indicated the potential for reduced vibration response in this articulated rotor if the first elastic flatwise and edgewise frequencies could be tuned to the range of 3.2 to 3.5/rev and 5.5 to 5.7/rev, respectively. These studies also showed shaping of the first and second elastic flatwise modes to be of prime importance. Thus, the overall objectives of the design problem were to meet the specified frequency criteria, to drive the first two flatwise modal integrals with cubic weighting to zero, and to maintain about the same blade weight if possible. The second flatwise frequency and the first edgewise modal integral were monitored but not included in the performance index.

The automated design procedure was used to achieve an optimized design (modified Design A) having the desired dynamic characteristics shown in Fig. 13. As shown in this figure, the automated design procedure met all the criteria specified for the primary vibration parameters. Furthermore, these significant changes in dynamic characteristics were achieved while allowing only a 4 percent increase in blade weight. In order to obtain this design, blade weight was added to the performance index to be minimized along with the frequency and modal shaping criteria. In addition to practical upper and lower bounds placed on each design variable, constraints were applied to the first two flatwise modal integrals to emphasize their importance and to ensure satisfaction of a threshold value of  $\pm 0.005$ . Note that this value corresponds to the dashed line shown in Fig. 13 and represents reductions of eighty and ninety percent in the first two flatwise modal integrals, respectively. As added benefits, the second flatwise frequency was driven away from 5/rev and the first edgewise modal integral was reduced by over 95 percent.

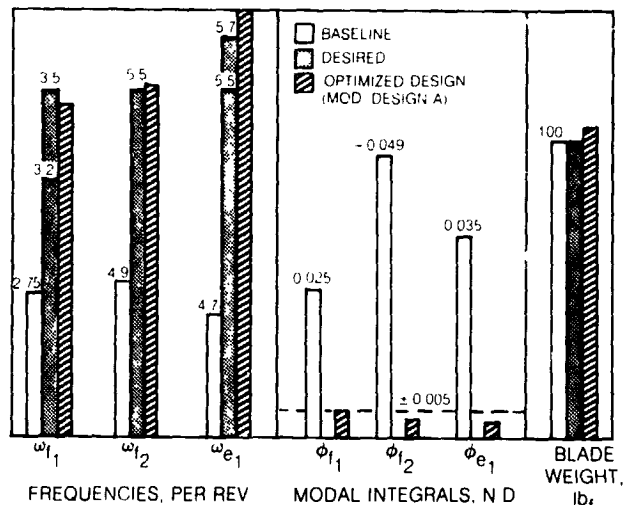


Fig. 13. Dynamic Characteristics of the Baseline and Optimized Blade Designs

Figure 14 compares the final mass distribution for the optimized blade design (modified Design A) to the distribution for the baseline production blade. The cross-hatched region represents blade root-end hardware which was not modified. While the blade weight for both the production blade and the optimized design were about the same, the mass distributions were significantly different. The automated design procedure shifted almost 15 lbs from mid-span to the outer 25 percent of the blade. This was required to achieve the substantial increase specified in the first flatwise natural frequency. As an added benefit, the increased mass outboard also improves rotor auto-rotation characteristics. About a 40 percent increase in edgewise stiffness across most of the blade span was required to achieve the high frequency specified for the first elastic edgewise mode. Changes made by the analysis in flatwise structural stiffness

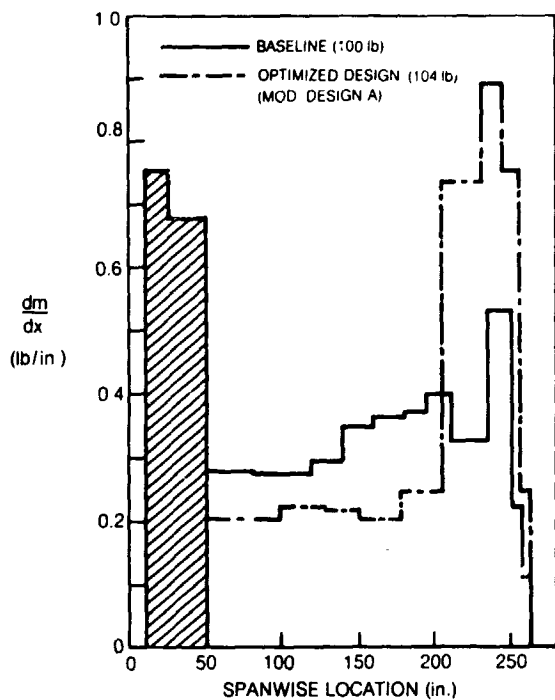


Fig. 14. Comparison of Mass Distributions for Baseline and Optimized Blade Designs

along the blade span were insignificant, since flatwise frequency and mode shape requirements were accomplished through changes in the spanwise mass distribution.

The vibration characteristics for the optimized blade design determined by the simplified automated design procedure were verified in G400. These characteristics were presented in Figs. 2 and 3 and were discussed in the section on blade design for reduced vibration. In summary, the two inplane hub shear components were reduced by over 65 percent and the vertical shear by 20 percent. As a result, predicted reductions in vibration on the order of 50 percent were achieved in cockpit and cabin vibration.

Furthermore, significant reductions in flatwise and edgewise bending stresses and in torsional stress all along the blade span were predicted. Reductions of nearly 50 percent were achieved at all the critical stress areas (outboard flatwise, midspan edgewise, and inboard torsional) despite the lack of stress constraints and stress terms in the performance index.

#### Closed-Loop Higher Harmonic Control

The use of a self-adaptive controller to implement higher harmonic control (HHC) in closed-loop fashion potentially allows significant vibration reduction to be achieved throughout the flight envelope. In this approach, higher harmonic blade root pitch, which can be input through the standard swashplate configuration, is used to modify blade airloads and reduce harmonic blade forcing of the

fuselage. Reference 20 presents an excellent review of past analytical and experimental work in helicopter higher harmonic control. More recently, the concept of closed-loop HHC has been successfully demonstrated in flight tests (Ref. 21).

In recent years, UTRC has focused on the analytical development, evaluation, and refinement of closed-loop self-adaptive higher harmonic control algorithms. References 22 and 23 present the results for a numerical simulation of a closed-loop deterministic control algorithm. The simulation was based upon a Black Hawk (UH-60) aircraft flying at various steady flight conditions. References 7 and 8 present the results of a more recent analytical study involving a simulation of the H-34 rotor mounted on the NASA Ames Rotor Test Apparatus (RTA) of the 40 x 80 ft wind tunnel. This investigation involved the refinement and evaluation of alternative controller configurations in order to compare their performance and to more fully understand the effects of tuning parameters within the algorithms. A generic controller computer code was developed to give the capability to readily define many different algorithms by selecting from three control approaches (deterministic, cautious, and dual), two linear system models (local and global), and several methods of limiting control. The generic controller is currently being used in analytical studies in preparation for open- and closed-loop flight tests of the Sikorsky S-76 (Ref. 24). An overview of the generic controller, analytical simulation of closed-loop control, and results presented in detail in Ref. 7 is given below.

#### Generic Active Controller

Figure 15 shows the computer simulation used to evaluate and compare the performance of the alternative algorithms included in the generic active controller. This simulation of closed-loop control is achieved by linking the generic controller to a nonlinear aeroelastic analysis (G400), which simulates the rotorcraft by calculating the

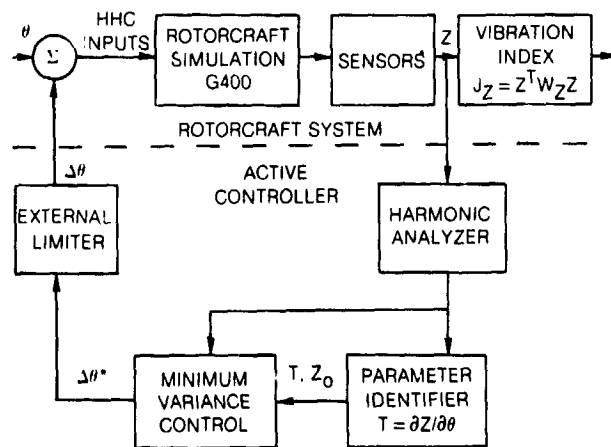


Fig. 15 Simulation of Active Vibration Control System

vibration response at a set of fixed-system sensor locations. Based on this response and on-line identification of system parameters, the active controller calculates and commands the HHC inputs required to further reduce vibration in the fuselage. These commanded inputs are imposed on the rotor by the G400 analysis with the inputs prescribed by the rotating system components (i.e., 3, 4 and 5 per rev). For computational efficiency, a constant inflow model has been used in G400. No measurement noise was simulated in this initial investigation.

Regardless of the control approach or system model implemented by the generic controller, there are two fundamental characteristics of the active controller: (1) a quasi-static linear transfer matrix (T-matrix) relationship between the vibration response and the HHC inputs is assumed and (2) the T-matrix is identified on-line to account for changes due to system nonlinearities or variations in flight condition. Each control approach can be based on one of two system models. The local model linearizes the system T-matrix about the current vibration response, Z, while the global model linearizes about the uncontrolled vibration level, Z<sub>0</sub> (zero HHC), which must also be identified.

As shown in Fig. 15, accurate identification of the T-matrix, as well as Z<sub>0</sub> for the global model, is important for good vibration reduction, since the minimum variance control algorithms all depend explicitly on the estimates of these parameters. The method used for estimating and tracking these system parameters is discussed in detail in Ref. 7. In short, each row of the T-matrix is considered to be a time-varying state vector, which is tracked by a Kalman filter identification algorithm.

Once system identification is completed, the required change in control for minimum vibration in the ith control update is calculated by a minimum variance control algorithm (Ref. 7). This algorithm is based on minimization of a quadratic performance index that consists of a weighted sum of the squares of the input and output variables. The performance index can be written in matrix notation as follows:

$$J = Z_i^T W_Z Z_i + Y_i^T (\beta \cdot \lambda \cdot P_i) W_{Zjj} Y_i + \theta_i^T W_\theta \theta_i + \Delta \theta_i^T W_{\Delta \theta} \Delta \theta_i \quad (1)$$

where  $Y_i = \Delta \theta_i$  for the local model and  $Y_i = (\theta_i^T \ 1)^T$  for the global model. The index  $\beta$  acts as a switching function dependent on the control approach used. The performance index J is a function of not only the vector of computed harmonics of vibration (Z), but also the vector of pitch control inputs ( $\theta$ ) and incremental change in control ( $\Delta \theta$ ). In the first term,  $W_Z$  is a diagonal weighting matrix used to reflect the relative importance of each vibration component. This term, referred to later as the vibration index, is indicative of overall effectiveness in reducing vibration. The second term is used to modify the controller algorithms to account

for uncertainties in identified system parameters according to the underlying assumptions of the control approach being used. These uncertainties are reflected in  $P_i$ , the covariance matrix calculated by the Kalman filter identification algorithm. The effect of this stochastic control term is determined by  $\beta$ , and the arbitrary stochastic control constant  $\lambda$ . Finally, the last two terms use diagonal weighting matrices  $W_\theta$  and  $W_{\Delta \theta}$  to inhibit excessive control amplitudes and rates of change in control, respectively. This "internal limiting" is used not only to satisfy hardware requirements, but also to enhance controller performance.

For the deterministic control approach,  $\beta$  is set to zero, since all system parameters are assumed to be explicitly known despite the fact that only estimates for the T-matrix are available. In the cautious approach, it is recognized that some of the system parameters are only estimates, and control inputs are implemented more cautiously than for the deterministic approach. This is accomplished by setting  $\beta$  equal to one. The resulting positive stochastic control term has a similar effect to that of  $W_{\Delta \theta}$  or  $W_\theta$ , depending on the system model, but is dependent on the uncertainty in the identified T-matrix, as reflected by  $P_i$ . In the dual control approach, an attempt is made to improve long term system identification by actively probing the system, while maintaining good control. In the generic controller, this is achieved with a negative value for  $\beta$ . The effect, analogous to reductions in weighting placed on control inputs, causes the system probing inherent to the dual controller. Whereas the cautious controller penalizes control when identification is poor, the dual controller increases control.

Finally, Fig. 15 shows that the active controller externally limits the optimum control inputs calculated by the minimum variance control algorithm before implementing new inputs in the rotorcraft simulation. This is referred to as external limiting since it is done outside the minimum variance control algorithm and without regard to optimality of the resulting solution. With external limiting, satisfaction of absolute control limits can be ensured. In contrast, internal limiting, which is accomplished by appropriate tuning of the weighting matrices,  $W_\theta$  and  $W_{\Delta \theta}$ , takes into account the desire to inhibit magnitudes and rates of change of control while calculating the optimum solution.

#### Analytical Results

The aeroelastic simulation of the rotorcraft in Refs. 7 and 8 was based on a fully articulated, four-bladed H-34 rotor mounted on the Rotor Test Apparatus (RTA), which is used to represent the fuselage in full scale rotor tests in the NASA Ames 40 x 80 ft wind tunnel. Vibration response information was calculated at six locations in the RTA. These components included three orthogonal directions (vertical, longitudinal, and lateral) and

were spread throughout the RTA (nose, main cross-beam, and tail).

A steady level-flight condition was selected for the initial tuning and evaluation of all primary controller configurations. This baseline condition had a forward velocity of 150 kt and a nominal value of 0.058 for  $C_T/\sigma$  (8250 lb thrust). Based on these results, a representative controller configuration was selected and tuned for each of the three control approaches. All three controllers were based on the global system model. The deterministic controller used internal weighting on  $\Delta\theta$  with  $W_{\Delta\theta}$  to maintain an acceptable rate of change of control. The cautious controller used neither external nor internal  $\Delta\theta$  limiting, but inherently slowed down the implementation of control via the stochastic control term. The dual controller used external rate limiting to allow the inherent perturbations in control inputs to occur without excessively compromising short term control. The performance of these controllers were subsequently evaluated at several steady flight conditions and during several short duration maneuvers as discussed below.

Steady Level Flight Conditions - Figure 16 presents the G400 predicted results for each of the three controllers operating closed-loop at the baseline flight condition. The simulation included three revs of uncontrolled flight to allow initial numerical transients to die out before activating each controller at rev 4. Figure 16 shows predicted time histories of the vibration index  $J_z$  and the amplitude of the 3 per rev HHC input commanded by each control approach. While not shown, 4 and 5 per rev inputs commanded by each controller had similar time histories. Since the vibration index is a weighted sum of the squares of all the vibration components being actively controlled, it is a good indicator of overall controller performance in reducing vibration. Note that the vibration index plotted involves only the first term shown in Eq. (1). While the other terms are important to overall controller performance and stability, they are not indicative of vibration reduction achieved by the controller.

Figure 16 shows that all three controllers did an excellent job of reaching a new steady vibration level that is greatly reduced from the uncontrolled vibration level at rev 4. After only two revs of active control, both the deterministic and cautious controllers achieved and maintained at least a 90 percent reduction in the vibration index. The dual controller required about 5 revs of active control to achieve the same level. By rev 10, all three controllers had essentially converged to a value of the vibration index that was only 3 percent of the uncontrolled value.

This figure also shows the time history of 3 per rev HHC amplitude commanded by the three controllers. The deterministic and cautious controllers smoothly increased the amplitude of all three control inputs, while continually reducing

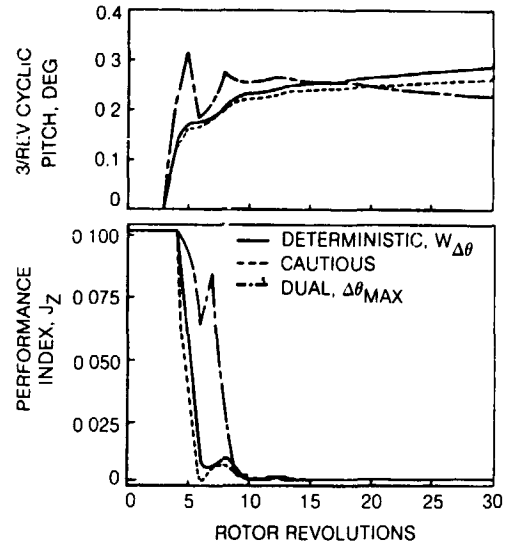


Fig. 16. Time History of Vibration Index and 3 Per Rev Control at Baseline Flight Condition ( $V = 150$  kt,  $C_T/\sigma = 0.058$ )

the vibration index. In contrast, the dual controller exhibited a tendency to probe the system by perturbing the higher harmonic cyclic inputs. This probing initially resulted in a slight degradation in short term control as can be seen in the vibration index. After identification improved, system probing diminished and the final controller solution was as good as that of the deterministic and cautious controllers. The dual controller's tendency to probe the system was somewhat inhibited by an application of external rate limits. Without these limits, the perturbation in control inputs used to probe the system were much larger and resulted in much worse short term control before converging to final solution.

Figure 17 compares the uncontrolled 4 per rev vibration levels at rev 4 to those at rev 30 with active control. All three controllers substantially reduced vibration at all locations except the two lateral components that had very low initial levels of vibration, which were maintained. Reductions in vibration for the four primary components were between 75 and 95 percent.

Also shown in Fig. 17 are the fixed system hub vibrations. Note that angular accelerations have been multiplied by 1 ft to be plotted in g's in this figure. The two largest contributors (vertical and longitudinal) were reduced by all three controllers. A substantial 75 percent decrease in the longitudinal component was achieved, while a more modest 20 percent reduction was achieved in the vertical component. The other four components, which were smaller initially, remained at about the same levels. The reductions in vibration in the RTA were achieved by a combination of reduced forcing at the rotor hub and vectorial cancellations of hub component contributions.

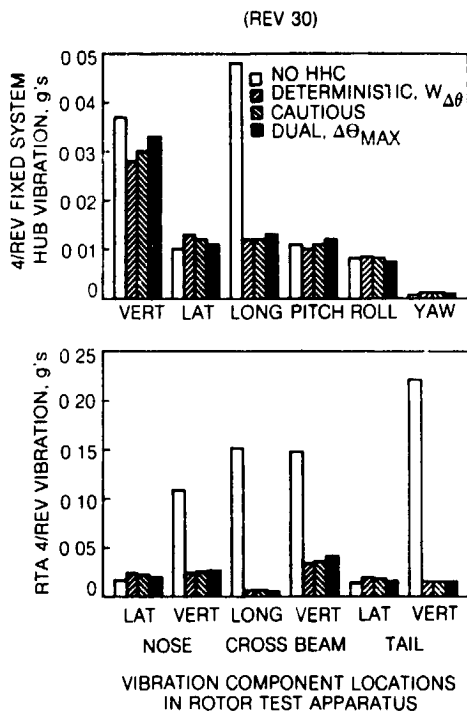


Fig. 17. Effect of Active Control on 4 Per Rev Vibration at Baseline Flight Condition ( $V = 150$  kt,  $C_T/\sigma = 0.058$ )

In addition to the baseline flight condition, each of the three controllers was also evaluated over a range of forward velocities from 112 to 150 kt at a nominal value of 0.058 for  $C_T/\sigma$  and over a range of rotor thrusts having values of 0.058 to 0.085 for  $C_T/\sigma$  at a velocity of 150 kt. Between 75 to 95 percent reductions in vibration were achieved by all three controllers at all steady flight conditions. These reductions in the individual components in vibration correspond to at least a 97 percent reduction in the vibration index at all steady flight conditions. Convergence to an acceptable control solution occurred quickly and smoothly. After 5 control updates, at least an eighty percent reduction in the vibration index was achieved and maintained. These results were obtained at all steady flight conditions with no retuning of the controller and with the same initial T-matrix developed and used at the baseline ( $V=150$  kt,  $C_T/\sigma=0.058$ ) flight condition. The required amplitudes of 3, 4, and 5 per rev control increased with both velocity and rotor thrust, but were each less than 1.0 degree for all steady flight conditions.

All the steady flight results presented above for the global system model are generally applicable to the local model as well. It was not until controller performance was evaluated during the short duration maneuvers discussed below that any significant difference in controller behavior due to system model was noticed. From the steady

flight conditions studied to date, no distinct advantage in terms of controller performance has been identified for either the deterministic or cautious control approaches. The dual controller, while equally effective in reducing vibration, tended to have worse short term control and somewhat more oscillatory behavior due to system probing. The baseline deterministic and cautious controllers were relatively insensitive to less than optimum tuning of internal parameters. However, it should be noted that the use of internal limiting in the deterministic approach dramatically improved controller stability and performance compared to that achieved with external limiting. The use of properly tuned internal weightings on control inputs significantly improved the deterministic controller performance according to all criteria: much greater vibration reduction in the first step of active control; faster convergence; significantly greater reduction in vibration at convergence; and smaller final control inputs. The dual controller was very sensitive to the tuning of  $\lambda$ . It remains to evaluate the effect of measurement noise on the performance of each control approach.

Short Duration Maneuvers - Each of the three controllers was also evaluated during several short duration maneuvers, while using the same initial T-matrix and tuning developed at the steady baseline condition. Each of the maneuvers involved an increase in rotor thrust from the initial steady baseline condition,  $C_T/\sigma = 0.058$ , via step and ramp changes in collective pitch during an otherwise steady flight condition at 150 kt. These changes in collective pitch resulted in 40 to 50 percent increases in rotor thrust relative to the baseline condition. After all transients subsided, the final flight condition corresponded to one of the steady flight conditions investigated (i.e.,  $C_T/\sigma = 0.08$  or 0.085). For each of these maneuvers, the active controllers remained stable, maintained peak vibration response well below uncontrolled levels, and reduced vibration to the same levels achieved at equivalent steady conditions. Retuning of the controllers was necessary to achieve satisfactory performance during some maneuvers. Without retuning, the local model was much more oscillatory and required more time to converge than the global model during maneuvers. This may indicate that the local model is more sensitive to tuning at different flight conditions or perhaps more sensitive to inaccurate vibration response information due to transient effects. Detailed results for the various steady flight conditions and short duration maneuvers are presented in Ref. 7. The results for the maneuvers investigated indicate the need for further evaluation during extended continuous maneuvers.

Blade Stresses and Rotor Performance - Increases in rotor blade stresses were noted at most flight conditions investigated. However, results also suggest that the penalty of increased vibratory blade loads may be reduced by tailoring of HHC inputs with unequal  $W_\theta$  weighting. It may

also be possible to alleviate the increases in stress, without compromising vibration reduction, by including appropriately weighted terms representative of blade stresses in the performance index shown in Eq. (1). While these approaches were not pursued, certain results did indicate that they might be feasible. For example, multiple control solutions resulting in similar vibration reductions, but having different effects on rotor blade stresses, were obtained. One such solution involved an arbitrary elimination of 5 per rev control at the highest thrust condition investigated. The result was relatively small increases in blade stresses and excellent reductions in vibration. The increase in blade stresses were much smaller than those where 5 per rev control was implemented, even though vibration reductions for both cases were comparable.

A degradation in rotor performance was also noted at many flight conditions. At the baseline condition, the application of HHC caused an increase in required torque on the order of 5 percent. An analytical study of the effect of closed-loop HHC on rotor performance should be performed when using a variable inflow model that includes unsteady aerodynamic effects. Again, it may be possible, if necessary, to guide the controller to better control solutions in terms of rotor performance, as well as vibration, by including a term indicative of rotor torque in the performance index.

#### Blade Appended Aeroelastic Device

In addition to alleviating vibration through blade design and active pitch control, the use of blade appended aeroelastic devices has been analytically explored at UTRC. One such device, as reported in Ref. 9, is a passive tuned tab shown in Fig. 18. The objective of this tab is to create harmonic airloading of favorable amplitude and phase to cancel the inherent harmonic airloading which acts as a source of main rotor vibration. Physically, the passive blade tab is appended near the trailing edge of a standard rotor blade by some hinge configuration so that the tab can deflect freely about the hinge. The hinge could be mechanical in nature with bearings or it could be made of a composite material that has a large allowable strain such that the tab is actually "taped" to the blade by the composite hinge. The latitude in selecting the spring rate of the tab would provide a dynamic tuning capability; the spring rate could be provided either mechanically or by the elasticity of the material for a composite hinge.

The basis of the concept, as described in Ref. 9, is as follows: when a rotor blade tab deflects, it creates an incremental airload and pitching moment on the rotor blade as a result of the increased camber. The pitching moment also creates an additional airloading on the rotor blade by elastic twisting to create an incremental angle-of-attack. The importance of this source of airloading is closely tied to the blade torsional stiff-

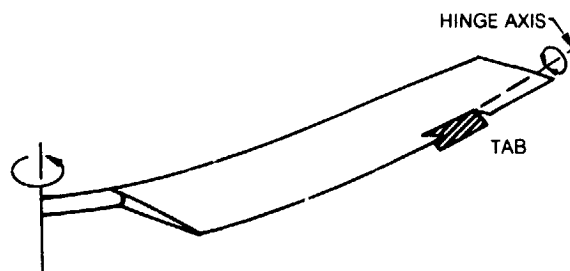


Fig. 18. Blade Vibration Control Device -- Passive Tuned Tab

ness and natural frequency, and is secondary to that obtained from the effective camber change for this concept. When the tab deflects harmonically, the airloads and pitching moment created by the tab deflection are also harmonic. Therefore, to derive benefit from the tab, the tab motion must be correctly phased to cancel the inherent harmonic airloading that excites the blade flatwise modes and produces vibration.

The driving forces on the tab are its own inertial loading as the blade flaps and pitches (rigid body and flexible motions) and the aerodynamic forces arising from blade and tab motion. By increasing the offset of the tab center of gravity from the hinge, the inertial forcing can be increased. For a tab located at the blade tip, most of the vertical harmonic motion would come from the response of the flexible flatwise modes and nearly all of the torsion motion would be due to the response of the blade first torsion mode. Hence, there is a direct relationship between the motion that is inertially forcing the tab to deflect and the vibration that is a result of that same motion. Therefore, the success of this concept depends on correctly sizing and placing the tab along the rotor blade span and choosing its mass and natural frequency to achieve the maximum vectorial cancellation of inherent harmonic airloading.

An initial analytical evaluation of this concept has been conducted (Ref. 9) using the G400 rotor aeroelastic analysis (Ref. 6), together with data for a realistic helicopter rotor blade (UH-60A, Black Hawk) in high speed flight (175 kts). Variations in tab mass, frequency, and center-of-gravity location were investigated for two tab spanwise locations. While some modest reductions in the inplane components (longitudinal and lateral) of vibratory hub shear were predicted, unacceptable increases in the vertical component have been predicted for the blade/tab as configured in the study. The reason for the vertical shear increase remains to be determined before any further investigation to determine if other configurations have potential for overall vibration reduction.

#### Vibratory Airloads

An ongoing activity at UTRC has been directed toward the development of helicopter airload meth-

odology and the advancement of the understanding of vibratory airloads of the rotor and fuselage. A representative sampling of results of this activity are presented in Refs. 10 to 19. This activity has included investigations of rotor wake and airflow, unsteady airloads related to dynamic stall, blade airload coupling with blade response and aeroelastic flexibility, and both rotor/fuselage and rotor/empennage interactional aerodynamics.

#### Wake Induced Blade Airloads

A recent investigation of helicopter rotor wake geometry and its influence in forward flight is reported in Refs. 10 and 11 and summarized in Ref. 12. This analytical investigation was conducted to generalize the wake geometry of a helicopter rotor in forward flight and to demonstrate the influence of including wake deformation in the prediction of rotor airloads and performance. Predicted distortions of the tip vortex of each blade relative to the classical undistorted geometry were generalized for vortex age, blade azimuth, advance ratio, thrust coefficient, rotor disc attitude, and number of blades based on a representative blade design. A computer module and charts (Ref. 11) were developed for approximating wake geometry and identifying wake boundaries and locations of blade-vortex passage. Predicted H-34 rotor airloads for several rotor inflow/wake models were compared with test data for several flight conditions.

An example of the tip vortex geometry in forward flight (30 kts), as predicted by the UTRC Wake Geometry Analysis (Ref. 13), is shown in Fig. 19. A sample isometric view of distorted tip vortices from the generalized wake model is shown in Fig. 20. The characteristic wake distortion features observed from experimental results are present in the predicted tip vortex geometries. The forward and lateral sides of the wake are distorted toward the rotor relative to the undistorted wake model. This results in close blade-vortex passages which can introduce severe local azimuthal and spanwise gradients in blade airloads which are not predicted with uniform inflow and undistorted wake (rigid wake) analytical models. This is shown in Fig. 21 where the predicted airloads (blade lift distributions) based on the different inflow/wake models are presented in the form of surface contour plots. As indicated, inclusion of tip vortex deformation in the wake model results in increased higher harmonic content in the airload prediction. The outboard advancing side of the rotor typically exhibits the most severe vibratory airload gradients with significant but lesser variations on the outboard retreating side. This is exemplified in the H-34 airload test data shown in Fig. 22, taken from Ref. 10, as acquired at 48 kts (0.129 advance ratio) in flight test (Ref. 25).

Typical of low speed transition conditions, a sharp "down-up" impulse is applied to the tip region of the advancing blade and an "up-down" impulse is applied to the tip region of the

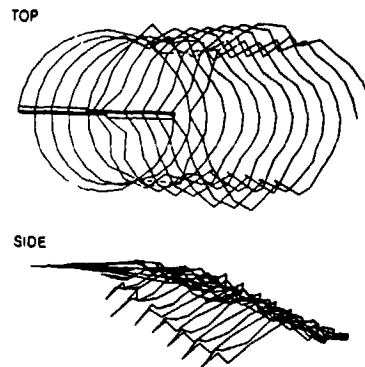


Fig. 19. Predicted Distorted Tip Vortex Geometry

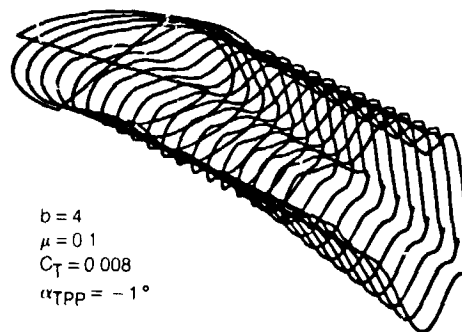


Fig. 20. Isometric View of Generalized Distorted Tip Vortices

retreating blade (Fig. 22). For higher speed flight the vibratory airloads are concentrated at the outboard region of the advancing side where a characteristic "up-down" impulse occurs. This is exemplified in Fig. 23 where the airloads are shown for the H-34 rotor operating at 110 kts (0.29 advance ratio), as measured in a wind tunnel (Ref. 26). These airload characteristics have been shown by Hooper (Boeing-Vertol) in Ref. 27 to be surprisingly consistent for different helicopters with substantial differences in size, trim, and number of blades per rotor. In this reference, the combined higher harmonic components of airloading (harmonics 3-10) are plotted for several aircraft and, with some exceptions at high speed, these vibratory components are shown to be characteristically consistent.

The ability to predict the vibratory airloading characteristics is depicted in Fig. 22 from Refs. 10 and 12, where the results of combining the Sikorsky Generalized Performance Analysis (airloads), the UTRC Rotorcraft Wake Analysis (induced airflow), and the UTRC Wake Geometry Analysis (distorted wake) are presented for the H-34, 48 kt condition. The general ability to predict the induced airflow of the rotor wake in the vicinity of the blades is shown through comparisons with laser velocimeter and other test data in Refs. 15 and 16. The influence of wake distortions on blade

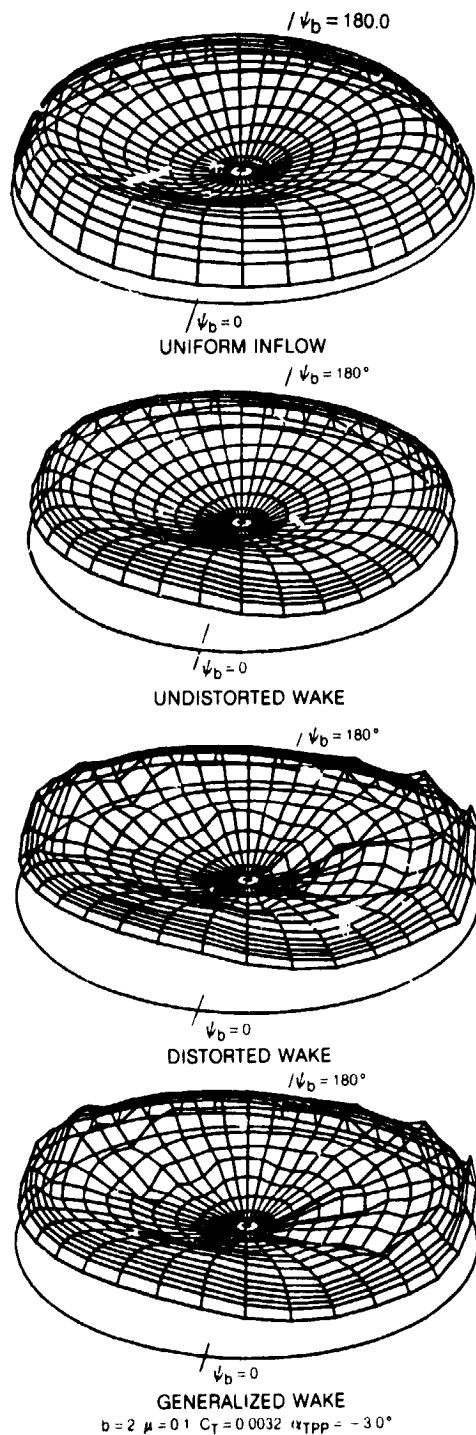


Fig. 21. Blade Lift Distributions Predicted with Various Wake/Inflow Models

airloads is described in these references to be related to the degree of proximity of the tip vortices to the rotor blades and the number of locations of close blade-vortex passages. For steady level flight, the wake influence generally increases with decreasing advance ratios, decreasing disc attitude and increasing number of blades. The

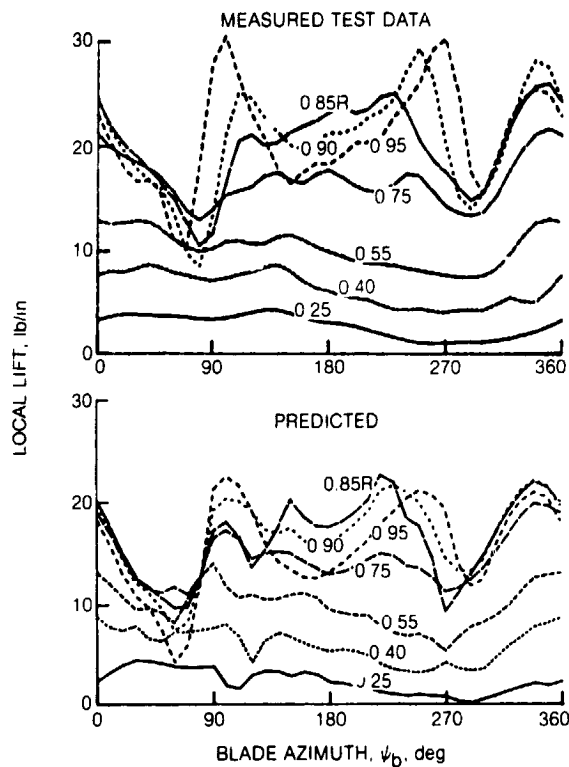


Fig. 22. Measured and Predicted Blade Airloads. (H-34, 48 kts)

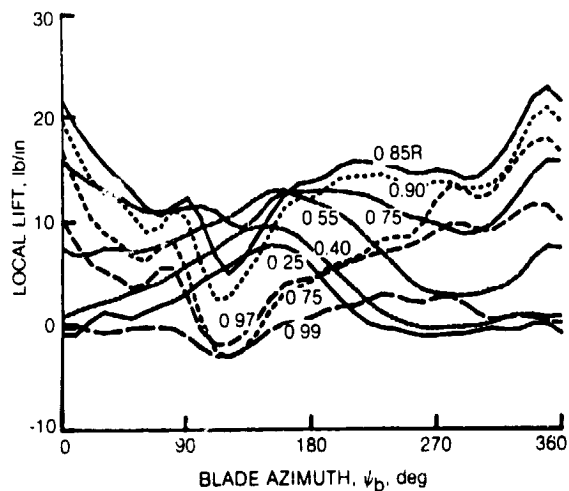


Fig. 23. Measured Blade Airloads. (H-34, 110 kts).

wake distortions and related airload influence are most complex at low advance ratios, where the difficulty of accurate wake geometry and airloads prediction is compounded by the larger number of close blade-vortex passages and by blade-vortex impingement due to the movement of the tip vortices above and then down through the rotor disk.

The prediction of tip vortex distortions, which are in close proximity to the blades at localized regions of the rotor, results in a high sensitivity of predicted airloads to small differences in tip vortex geometry and the theoretical blade-vortex aerodynamic interaction model used. This sensitivity is demonstrated in Refs. 10 and 12. For example, the airload predictions in Fig. 22 resulted from the use of an expanded vortex core model to simulate vortex bursting near close blade passages. Both higher and lower amplitudes of vibratory airloading on the advancing and retreating sides were predicted with other vortex core models and small variations in wake geometry (blade-vortex spacing). Although the need for further analytical refinement is evident, the degree to which the analysis, with a distorted wake model, was able to reproduce the measured airload distributions is encouraging and indicative that, with future emphasis on blade-vortex interaction modeling, wake methodology has the potential to provide a useful predictive tool for vibratory airloads.

Wake geometry and blade-vortex intersection plots in Refs. 10 and 27 indicate the source of the impulsive type airloads on the advancing and retreating sides to be at least partially attributable to close blade-vortex interaction. It is shown that the blade passes close to a nearly parallel tip vortex from a preceding blade in the first quadrant and the fourth quadrant of the rotor. At higher flight speeds, where the vibratory airloading is predominantly on the advancing side, the vibratory airloads are caused by a combination of blade-vortex interaction, blade motions, and the characteristic blade "Mach tuck" phenomenon. This phenomenon is known to result from the aft movement of the blade aerodynamic center, due to compressibility, which results in a nose down pitching moment for positive lift and a corresponding blade torsional deformation. This produces a negative azimuthal gradient in blade lift. Blade sweep has been used to counter this effect in the advancing side negative lift region. In Ref. 27, it is hypothesized that the "up-down" impulse on the advancing side at high speed conditions is opposite to the "down-up" impulse at lower speeds due to the opposite direction of vorticity produced by the negative lift region at the tip at high speed. In high speed flight, vibratory airloads on the retreating side can also be caused by dynamic stall as shown and predicted in Ref. 18.

#### Airloads From Blade Motions

The mechanism by which vibratory airloads couple with blade motions and modal response are described in Ref. 1. A primary source of vibratory airloads in forward flight is the interharmonic coupling of airloads and blade response that increases with forward speed. As mentioned earlier, the phenomenon can be viewed as a cascade effect (Fig. 1), starting with the basic characteristic of helicopter rotors in forward flight. One per rev airloads are created by either blade flap-

ping or cyclic pitch. The one per rev airloads cause one per rev response of the blade modes. The resulting one per rev motions create 2 and 3 per rev airloads. These airloads in turn cause 2, 3, 4, and 5 per rev response of the blade modes and so on. Different blade modes respond more than others due to resonant type responses, and cause vibration from the combination of inertial, elastic, and direct airloading. Thus, significant vibratory airloads are created by blade motions and elastic response as well as wake induced, compressibility, and dynamic stall effects.

#### Interactional Rotor-Fuselage Airloads

In order to accurately predict coupled rotor-fuselage vibrations, it is necessary to consider the aerodynamic interaction of the individual components of the helicopter. In Ref. 17 it is shown that the presence of the fuselage distorts the rotor airflow and wake causing two-per-rev as well as other harmonic airload excitations at the rotor. Examples from Ref. 17 of the calculated effect of the airframe presence on the rotor inflow velocities and inner blade angle-of-attack distribution are shown in Fig. 24. Here, the influence of the fuselage on the rotor inflow velocities ( $\Delta V_N$ ) is shown as predicted using the Sikorsky fuselage panel method (WABAT) for a relatively low rotor

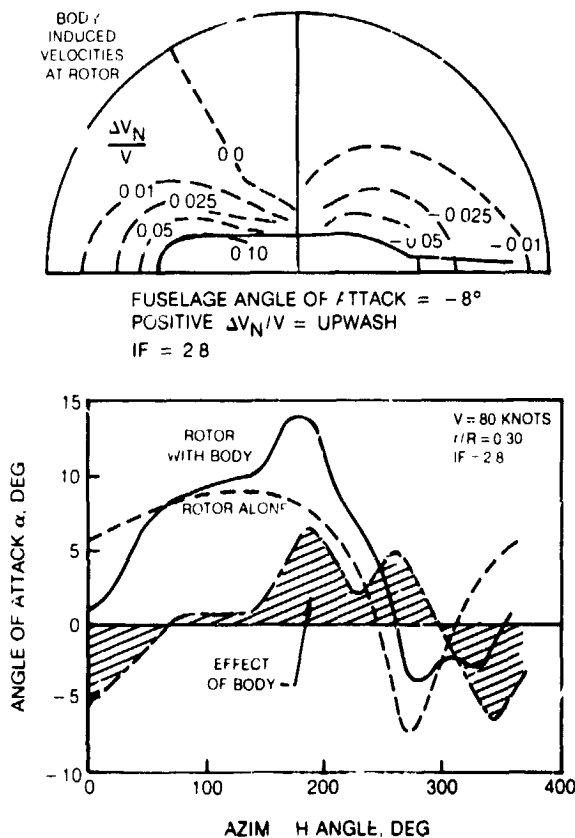


Fig. 24. Predicted Body Induced Velocities at Rotor Plane and Body Effect on Rotor Angle of Attack Distribution

configuration (IF=2.8). (The interference factor, IF, defined in Ref. 17, is representative of the ratio of the fuselage upper surface area to the rotor hub to fuselage distance.) The perturbation of the flow field at the rotor disc produces changes in the blade local angle-of-attack distributions which influence the blade response and airloads. Also in Fig. 24, the angle-of-attack distribution at one radial station is presented as predicted using the UTRC Rotorcraft Wake Analysis coupled with the Sikorsky Generalized Rotor Performance Analysis. In addition to two-per-rev, there is a significant third harmonic content in the increment representing the body induced effect. For low rotor configurations, this should be considered in computations of the vibration spectrum.

The influence of the rotor airflow on fuselage vibratory airloading must also be considered. Experimental results have indicated that the rotor blades and wake can produce significant oscillating fuselage pressures at principally the fundamental blade passage frequency. These pressure pulses have been recognized as a fuselage vibration mechanism, but this mechanism and its effect have not been fully investigated analytically. Methodology is currently being developed at UTRC to approximate the rotor wake deformation due to the fuselage and to calculate the unsteady fuselage pressures.

#### Interactional Rotor - Empennage Airloads

The Rotorcraft Wake Analysis and laser velocimeter measurements have been used at UTRC to demonstrate the significant influence of the rotor wake on fluctuating flow velocities in the vicinity of tail surfaces (Ref. 16). More recently, a computer program (RJEVA) has been developed that predicts the unsteady airloads that are imposed on the empennage surfaces due to its aerodynamic interaction with the main rotor wake (Ref. 19). A rotor wake program is used to determine the position and the strength of blade tip vortices that pass near the empennage surfaces. A nonlinear lifting surface analysis is utilized to predict the aerodynamic loads on the empennage surfaces in the presence of these concentrated vortices. The nonlinear analysis was formulated to include pertinent effects such as suction effects of the interacting vortices and the effects of time-variant shed vorticity behind the empennage surfaces. The problem is solved in a stepwise manner (time-domain); that is, a period corresponding to one blade passage is divided into a large number of time intervals and empennage unsteady airloads are computed at each time step. The output of the analysis consists of chordwise and spanwise airload distributions at each time step. These airload distributions are converted into harmonic airloads that can be applied to excite the tail boom in a vibration analysis. The results of a limited correlation study involving the application of the computer program to a full-scale helicopter stabilizer indicate an encouragingly good correlation between the analytical vibratory airload predictions and flight

test data. Sample results are shown in Fig. 25 for the 6 per rev airloads of the CH-53A horizontal stabilizer that are induced by the wake of the six-bladed rotor at a high speed condition (159 kts).

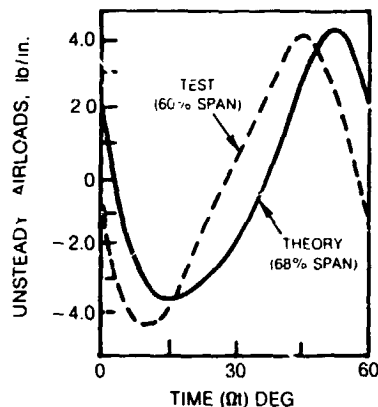


Fig. 25. Unsteady Airloads Induced by Rotor Wake on Empennage Lifting Surface

#### Concluding Remarks

Analytical studies have demonstrated the potential of various approaches to alleviate helicopter vibration. The approaches described herein should be considered to be complementary rather than entirely competitive. Blade design for vibration is the most desirable approach if vibration reduction can be achieved throughout the flight regime without penalties in performance, stresses, and weight. However, it may still be necessary to complement design optimization with other approaches such as active higher harmonic control to achieve the industry goal of 0.1 g vibration levels.

A blade design study has been conducted to identify important contributing components and establish appropriate vibration criteria. The availability of optimization techniques makes the design process more tractable and allows new designs that satisfy specified design criteria to be achieved in a much more efficient fashion than is possible in the traditional design process. As a result, it is possible to pursue more sophisticated design criteria and to achieve designs previously unobtainable. Since it is computationally inefficient to base a closed-loop design optimization procedure on a forced response analysis, vibration criteria based on blade modal properties have been developed. Results from the closed-loop analysis are then verified in a forced response analysis. Results of the blade design study for a high speed cruise condition indicate the potential for developing enhanced blade designs that can offer significant reductions in baseline vibration without resorting to special vibration alleviation devices, radical blade geometries, or weight penalties. Efforts to define further vibration criteria are underway.

Analytical studies have also demonstrated the potential for active higher harmonic control to reduce helicopter vibration. The results of the generic controller study indicate the potential for various control approaches to reduce vibration by 75 to 95 percent with small blade pitch amplitudes at a range of moderate to high speed and thrust conditions. Good controller performance was also demonstrated during short duration maneuvers. However, the potential for adverse effects on blade stresses and rotor performance was noted at many flight conditions. Analytical investigations are planned to determine the drivers of these effects and to develop methods for their alleviation.

The results for a passive tuned tab have been somewhat disappointing, with increases in some vibration components occurring at the same time that reductions in other components are achieved. Further investigation of blade appended devices, such as the passive tuned tab, is required.

Computerized analyses have been used as diagnostic tools to acquire a better understanding of the fundamentals of vibration by tracing the principal sources of vibration and loads and identifying the important contributing components. These analyses have also been used in simulating closed-loop higher harmonic control and in verifying the results of blade design changes or the effects of blade appended devices. Since the analyses remain to be validated, qualitative results regarding dynamic trends and characteristics of the rotor should be accepted more than quantitative results. The predicted absolute vibration and load levels are approximate as are the predictions of all other forced response helicopter analyses in use today. Significant progress has been made toward establishing a blade design procedure, and preparations for model tests to provide vibration data are underway.

Recent advancements of aerodynamic analytical tools are providing an understanding of the sources of vibratory airloads. Although further analytical refinement is continuing, the degree to which the distorted wake model is able to predict measured airloads is encouraging. Indications are that, with future emphasis on modeling blade-vortex interaction, the combination of distorted wake and aeroelastic response methodologies has the potential to provide a useful predictive tool for vibratory airloads.

#### Acknowledgements

The authors especially acknowledge the contribution of Robert B. Taylor who, as Supervisor, Advanced Rotorcraft Concepts and Dynamics, directed the vibration research activity within the Aeromechanics Research Section while he was at UTRC. He initiated the active higher harmonic control activity (Refs. 22 and 3), and conceived the passive tab vibration alleviation device. His work on blade design for vibration reduction (Ref. 1) provided the technical material for that section

of this paper. The contributions of T. Alan Egolf, Aeromechanics Research, UTRC, to results reported in the vibratory airloads section is also acknowledged. Dr. Richard L. Bielawa analyzed the passive vibration alleviation devices reported herein from Ref. 9, and Santu T. Gangwani developed the empenage analysis (Ref. 19).

The work reported herein was supported by the NASA Ames and Langley Research Centers, the U.S. Army Research and Technology Laboratories, and the United Technologies Corporation.

#### References

1. Taylor, R. B.: Helicopter Rotor Blade Design for Minimum Vibration. NASA Contractor Report 3825, (USAAVSCOM Report No. 84-A-2), August 1984.
2. Taylor, R. B.: Helicopter Vibration Reduction by Rotor Blade Modal Shaping. Proceedings of the 38th Annual Forum of the American Helicopter Society, May 1982.
3. Davis, M. W.: Optimization of Helicopter Rotor Blade Design for Minimum Vibration. Proceedings of the Multidisciplinary Analysis and Optimization Symposium, NASA Langley Research Center, Hampton, VA, April 1984.
4. Madsen, L. E. and G. N. Vanderplaats: COPES--A Fortran Control Program for Engineering Synthesis. Naval Postgraduate School, NPS69-81-003, March 1982.
5. Vanderplaats, G. N.: CONMIN--A Fortran Program for Constrained Function Minimization; User's Manual. NASA TMX-62, 282, August 1982.
6. Bielawa, R. L.: Aeroelastic Analysis for Helicopter Rotors with Blade Appended Pendulum Absorbers - Program Use's Manual. NASA CR-165896, June 1982.
7. Davis, M. W.: Refinement and Evaluation of Helicopter Real-Time Self-Adaptive Active Vibration Controller Algorithms. NASA Contractor Report 3821, September 1984.
8. Davis, M. W.: Development and Evaluation of a Generic Active Helicopter Vibration Controller. Proceedings of the 40th Annual Forum of the American Helicopter Society, May 16-18, 1984.
9. Bielawa, R. L.: Analytic Investigation of Helicopter Rotor Blade Appended Aeroelastic Devices. NASA Contractor Report 166525, February 1984.
10. Egolf, T. A., and A. J. Landgrabe: Helicopter Rotor Wake Geometry and Its Influence in Forward Flight, Volume I - Generalized Wake Geometry and Wake Effect on Rotor Airloads and Performance. NASA CR-3726, October 1983.

11. Egolf, T. A., and A. J. Landgrebe: Helicopter Rotor Wake Geometry and Its Influence in Forward Flight, Volume II - Wake Geometry Charts. NASA CR-3727, October 1983.
12. Egolf, T. A., and A. J. Landgrebe: Generalized Wake Geometry for a Helicopter Rotor in Forward Flight and Effect of Wake Deformation on Airloads. Proceedings of the 40th Annual Forum of the American Helicopter Society, May 1984.
13. Landgrebe, A. J.: An Analytical Method for Predicting Rotor Wake Geometry. Journal of the American Helicopter Society, Vol. 14, No. 4, October 1969.
14. Landgrebe, A. J., R. B. Taylor, T. A. Egolf, and J. C. Bennett: Helicopter Airflow and Wake Characteristics for Low Speed and Hovering Flight from Rocket Interference Investigations. Proceedings 37th Annual Forum, American Helicopter Society, May 1981, pp. 51-65; also, Journal of the American Helicopter Society, Vol. 27, No. 4, October 1982.
15. Landgrebe, A. J., and T. A. Egolf: Rotorcraft Wake Analysis for the Prediction of Induced Velocities. USAAMRDL TR-75-45, January 1976. (Available from DTIC as AD A021 202.)
16. Landgrebe, A. J., and T. A. Egolf: Prediction of Helicopter Induced Flow Velocities Using the Rotorcraft Wake Analysis. Proceedings of the 32nd Annual Forum of the American Helicopter Society, March 1975.
17. Landgrebe, A. J., R. C. Moffitt, and D. R. Clark: Aerodynamic Technology for Advanced Rotorcraft. Journal of the American Helicopter Society, Vol. 22, Nos. 2 and 3, April and July 1977--Parts I (pp. 21-27) and II. Also, Proceedings of Symposium on Rotor Technology, American Helicopter Society, August 1976.
18. Gangwani, S. T.: Prediction of Dynamic Stall and Unsteady Airloads for Rotor Blades. Journal of the American Helicopter Society, October 1982.
19. Gangwani, S. T.: Determination of Rotor Wake Induced Empennage Airloads. Proceedings of the American Helicopter Society National Specialists' Meeting on Helicopter Vibration, November 1981.
20. Johnson, W.: Self-Tuning Regulators for Multicyclic Control of Helicopter Vibration. NASA Technical Paper 1996, March 1982.
21. Wood, E. R., R. W. Powers, J. H. Cline, and C. E. Hammond: On Developing and Flight Testing a Higher Harmonic Control System. Proceedings of the 39th Annual Forum of the American Helicopter Society, May 1983.
22. Taylor, R. B., F. A. Ferrar, and W. Miao: An Active Control System for Helicopter Vibration Control by Higher Harmonic Pitch, presented at the AIAA/ASME/ASCE/AHS 21st Structures, Structural Dynamics Conference, AIAA Paper 80-0672, May 1980.
23. Taylor, R. B., P. E. Zwicke, P. Gold, and W. Miao: Analytical Design and Evaluation of an Active Control System for Helicopter Vibration Reduction and Gust Response Alleviation. NASA CR-152377, July 1980.
24. O'Leary, J. J., S. B. Kottapalli, and M. W. Davis: Adaptation of a Modern Medium Helicopter (Sikorsky S-76) to Higher Harmonic Control. Presented at the 2nd Decennial Specialists' Meeting on Rotorcraft Dynamics, Ames Research Center, November 7-9, 1984.
25. Scheiman, J.: A Tabulation of Helicopter Rotor-Blade Differential Pressures, Stresses, and Motions as Measured in Flight. NASA TM X-952, March 1964.
26. Rabbott, Jr., J. P., A. A. Lizak, and V. M. Paglino: A Presentation of Measured and Calculated Full Scale Rotor Blade Aerodynamic and Structural Loads, USAAVLABS TR 66-31, July 1966. (Available from DTIC as AD 639 981.)
27. Hooper, W. E.: The Vibratory Airloading of Helicopter Rotors. VERTICA, Vol. 8, No. 2, 1984. Also, Proceedings of the Ninth European Rotorcraft Forum, Stresa Italy, September 1983.

DISCUSSION  
Paper No. 22

ANALYSIS OF POTENTIAL HELICOPTER VIBRATION REDUCTION CONCEPTS

Anton J. Landgrebe  
and  
Mark W. Davis

Ed Austin, U.S. Army Applied Technology Laboratory: Jack, I was wondering on your higher harmonic control work, first of all, what sort of a frame time were you using for updating your controller, and did you try investigations of various frame times to see what was necessary?

Landgrebe: As far as frame time, you're talking about azimuth?

Austin: Right, the computation time for the controller.

Landgrebe: That was basically going through a one rcv-type update. There was not that much done in [determining] the sensitivity. It seemed to be adequate--if we had not gotten good results, we would have looked at other updates.

Andy Lemnios, Kaman Aerospace: Jack, I'm absolutely delighted to have you relook at the dynamics end of blade design in addition to the aerodynamics end, because I think this is a very fertile area for some very serious vibration reductions. As you know, we feel very strongly about the proper inertial coupling among the various modes, and by doing so you can very strongly influence what happens to the hub shears and hub moments. Also we feel that the first flapwise frequency being above 3 per rev as we talked about last night, is a very important parameter to design for. I did have a couple of questions for you. In your look at loads being transmitted to the fuselage from the rotor, did you also include the pitch link loads in that analysis?

Landgrebe: No, that was not included.

Lemnios: Typically, I know that in some helicopters, for example, those pitch link loads can account for 25 to 30% of the excitation forces. They're very significant and they cannot be ignored.

Landgrebe: Yes, we recognize that. They have been looked at in other studies as far as our unsteady aerodynamics studies, and you're right, they can be quite formidable.

Lemnios: The second question I had was, in this particular model did you have a lead-lag damper on this or not, or was it a bearingless rotor that you were looking at? Do you remember?

Landgrebe: In which study, in the vibrations study?

Lemnios: The vibrations study, yes.

Landgrebe: That was basically an S-76 type articulated blade.

Lemnios: The reason I ask is, did you put in the appropriate frequency characteristics of the lag damper? I know from our experience, lag dampers typically have a very uniform damping characteristic, and essentially zero spring rate, at the low frequencies; but that lag characteristic falls off, and the spring rate builds up to a liquid spring at the 4 and 5 per rev frequency and by ignoring the 5 per rev frequency, again you may be overlooking some significant vibratory forces.

Landgrebe: Bob [Taylor] can probably answer that question better than I can, but the point is that in the G400 analysis, there is a representation for the lag damper, but it doesn't take into account all the features that you have mentioned.

Bob Taylor, Boeing Vertol: I personally haven't seen any Sikorsky data or any other data at high speed where the 5 per rev vibration responses are important.

Lemnios: Strictly from our own experience, again, our frequency inplane is on the order of I think it was 5.4 per rev with the lag damper characteristics thrown in there, and that could be a significant contributor.

Taylor: I do believe that the [G400] model just used a linear lag damper.

Lemnios: Last but not least, the conclusion on your passive tuned damper may be appropriate, but you ought to also think about our favorite, which is a controlled tab instead of a passive tuned tab.

Peretz Friedmann, University of California, Los Angeles: I like the way you do the optimization with that modal-shaping type of concept. One of the things I was wondering--when you change the mass and stiffness distribution of your blade in order to reduce your vibration levels, you probably affect also the aeroelastic stability of the blades. Yet among the various constraints which you have enforced and listed in your slide, you had no aeroelastic stability constraint.

Landgrebe: That is correct, Peretz, that was not included within the constraint itself. The tack was taken to run the analysis and look to see if the analysis indicated any stability problems, which it did not. So that was not within the [constraint], but it could very well be put in in the future.

Friedmann: You miss the point of what the constraint means. It means that if you have a certain given aeroelastic stability margin, as a result of going through your procedure, that margin is not diminished. You still have a stable blade, yet you wouldn't like to trade off aeroelastic stability for vibration reduction of if you want to do it you should put some penalty on it.

Landgrebe: Obviously the concentration here was on vibration. I showed in one of the slides that really what you want to do is include performance, stability, loads, put them all in at the same time and that is the direction to go in, but we are not to that point yet.